

# A General Framework for Constructing Local Hidden-state Models to Determine the Steerability

Yanning Jia,<sup>1, 2, 3</sup> Fenzhuo Guo,<sup>1, 2, 3, \*</sup> Mengyan Li,<sup>1, 2, 3</sup> Haifeng Dong,<sup>4</sup> and Fei Gao<sup>3</sup>

<sup>1</sup>*School of Mathematical Sciences, Beijing University of Posts and Telecommunications, Beijing 100876, China*

<sup>2</sup>*Key Laboratory of Mathematics and Information Networks,*

*Beijing University of Posts and Telecommunications, Ministry of Education, China*

<sup>3</sup>*State Key Laboratory of Networking and Switching Technology,*

*Beijing University of Posts and Telecommunications, Beijing, 100876, China*

<sup>4</sup>*School of Instrumentation Science and Opto-Electronics Engineering, Beihang University, Beijing, 100191, China*

Not all entangled states can exhibit quantum steering, and determining whether a given entangled state is steerable is a crucial problem in quantum information theory. The main challenge lies in verifying the existence of a local hidden-state (LHS) model capable of reproducing all post-measurement assemblages generated by arbitrary measurements. To address this, we propose a machine learning-based framework that employs batch sampling of measurements and gradient-based optimization to construct an optimal LHS model. We validate our method by analyzing the steerability of two-qubit Werner and two-qutrit isotropic states. For Werner states, our approach saturates the analytical visibility bounds under three Pauli measurements, arbitrary projective measurements (PVMs), and arbitrary positive operator-valued measurements (POVMs). For isotropic states, we achieve the known analytical bounds under arbitrary PVMs. We further investigate the steerability of this class of states under arbitrary POVMs, and our results suggest that POVMs can offer an advantage over PVMs in revealing the steerability of such states.

## I. INTRODUCTION

Entanglement plays a central role in quantum information sciences [1]. Local measurements on entangled states can also arise other nonclassical correlations, such as quantum steering and quantum nonlocality, that cannot be replicated by any classical mechanism [2–4]. These nonclassical correlations have significant applications in information processing tasks [5–10]. Research has established that entanglement is a necessary condition for steering and nonlocality [11–16]. This means that entanglement alone is insufficient to guarantee these stronger nonclassical correlations. This raises a key question: how can we determine whether an arbitrary entangled state exhibits steering or nonlocality? Recently, Ref. [17] proposed a general method to determine the nonlocality of arbitrary entangled states, yet a general and effective framework for determining steerability remains lacking.

The concept of quantum steering was first proposed by Schrödinger [18], and was later rigorously formalized by Wiseman et al. [19]: In the semi-device-independent scenario, when the untrusted party performs arbitrary local measurements on an entangled state, if the resulting post-measurement assemblage obtained by the trusted party cannot be described by any local hidden-state (LHS) model, the assemblage is said to demonstrate quantum steering. An entangled state that allows the generation of one such assemblage is called steerable. Thus, determining the steerability of an entangled state essentially amounts to verifying whether there exists such an LHS model capable of describing all its possible post-measurement assemblages.

Several studies have analytically constructed LHS models for specific entangled states under different measurements, including symmetric states under projective measurements (PVMs) [19], arbitrary two-qubit states under PVMs [20], two-qubit Bell-diagonal and Werner states under general positive operator-valued measurements (POVMs) [21, 22]. For arbitrary quantum states, semidefinite programming (SDP) techniques were first applied to numerically search for LHS models under general measurements [23, 24]. However, these methods cannot establish general response functions applicable to arbitrary POVMs, and the constructed LHS models only describe assemblages corresponding to a finite set of sampled measurements rather than all possible POVMs. In recent years, machine learning has also emerged as a powerful numerical simulation tool and has been widely applied to problems in quantum information science [25–28]. Inspired by these advances, Ref. [29] employed neural networks (NNs) to characterize quantum steerability. Nevertheless, this approach faces the same limitation as the SDP methods. For the determination of steerability of two-qubit Werner states, the aforementioned SDP- and NN-based methods fail to saturate the known analytical bound.

In this work, we propose a machine learning-based framework for determining the steerability of a given entangled state under arbitrary measurements by constructing an LHS model. This framework effectively improves on the limitations of the previous numerical methods. By using batch random sampling of measurements, we efficiently traverse the entire measurement space. Through the expansion in orthonormal basis polynomials of the measurement space, we can use a finite set of hidden variables to establish general response function  $p(a|x, \lambda)$  for arbitrary measurement. Specifically,

\* [gfenzhuo@bupt.edu.cn](mailto:gfenzhuo@bupt.edu.cn)

the framework is implemented through an iterative process: at each step of the gradient descent, a new batch of measurements is sampled from the measurement space. For each batch, we first represent the response function  $p(a|x, \lambda)$ , and then construct the hidden state  $\sigma(\lambda)$  through a parameterization scheme. By combining these two components, we construct the corresponding LHS model. We define the average trace distance between the LHS assemblages and the quantum assemblages as the loss function. This loss function is minimized using gradient descent to update the parameters of the LHS model. Through repeated “sampling–evaluation–update” cycles, we ultimately obtain an optimal LHS model. When the loss function converges to zero, it indicates that the optimal model successfully reproduces the quantum assemblages, thereby certifying the quantum state as unsteerable.

To evaluate the effectiveness of our method, we applied it to analyze the steerability of two-qubit Werner states and two-qutrit isotropic states. For two-qubit Werner states, we obtained numerical visibility bounds consistent with analytical results under three Pauli measurements [30], arbitrary PVMs [20], and arbitrary POVMs [22]. For two-qutrit isotropic states, our numerical results achieved the analytical visibility bound under arbitrary PVMs [19]. For arbitrary POVMs, no precise analytical visibility bound for the steerability of this class of states is currently available. We therefore investigate the steerability numerically and find that the critical visibility is lower than that under PVMs. This observation indicates that POVMs offer a potential advantage over PVMs in revealing the steerability of these states.

## II. PRELIMINARIES

First, we provide a more detailed description of quantum steering and the LHS model in the simplest bipartite scenario. We consider a one-sided device-independent scenario: Alice’s side is the untrusted party, while Bob’s side is the trusted party.

In this setup, Alice and Bob share an unknown quantum state  $\rho_{AB}$ . Alice performs a local measurement labeled by index  $x$  chosen from some family  $\{M_{a|x}\}_{a,x}$ , with  $M_{a|x} \geq 0$  and  $\sum_a M_{a|x} = I$ . It should be noted that the measurements  $M_{a|x}$  performed by Alice are completely unknown to us. The possible post-measurement states for Bob’s system are given by the unnormalized state assemblage  $\{\sigma_{a|x}\}$  (see Fig. 1(a)). According to quantum theory, the elements of this assemblage can be obtained through the following expression:

$$\sigma_{a|x}^{QM} = \text{tr}_A [(M_{a|x} \otimes I) \rho_{AB}]. \quad (1)$$

A steering scenario can be fully characterized by this assemblage. The probability  $p(a|x)$  that Alice obtains outcome  $a$  given measurement  $x$  is calculated as  $p(a|x) =$

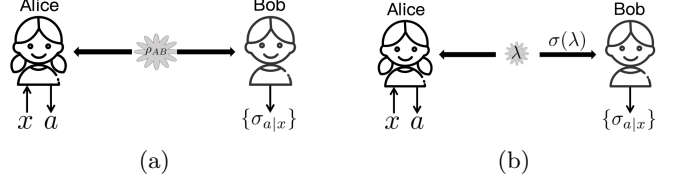


FIG. 1: Bipartite Scenarios. (a) The Steering Scenario: Alice and Bob share an unknown entangled state  $\rho_{AB}$ . Alice’s device acts as an untrusted black box, where the measurements  $M_{a|x}$  she performs are completely unknown; Bob’s side is trusted. We can determine whether Alice can steer Bob’s state by obtaining the assemblage  $\{\sigma_{a|x}\}$  from Bob’s side. (b) The LHS Model: This model describes a situation where a source sends a hidden variable  $\lambda$  to Alice and a corresponding hidden state  $\sigma(\lambda)$  to Bob, thereby generating the assemblage  $\{\sigma_{a|x}\}$ .

$$\text{tr}(\sigma_{a|x}^{QM}).$$

An LHS model refers to the situation where a source sends hidden variable  $\lambda$  to Alice and the corresponding hidden state  $\sigma_\lambda$  to Bob (see Fig. 1(b)). The unnormalized post-measurement state assemblage on Bob’s side is composed of the elements:

$$\sigma_{a|x}^{LHS} = \int d\lambda \mu(\lambda) p(a|x, \lambda) \sigma_\lambda, \quad (2)$$

where  $\mu(\lambda)$  is a probability density function over hidden variable  $\lambda$  shared between Alice and Bob, and  $p(a|x, \lambda)$  is a response function for Alice.

An given assemblage is said to demonstrate steering if it does not admit a decomposition of the form Eq. (2). Otherwise, the assemblage is unsteerable. An entangled state is steerable if and only if the assemblages obtained by arbitrary local measurements cannot be reproduced by any LHS model.

## III. THE CONSTRUCTION OF LHS MODEL

As we have defined the LHS model in the previous section, constructing such a model requires determining these three key components: the hidden-variable  $\lambda$ , the response function  $p(a|x, \lambda)$ , and the hidden state  $\sigma(\lambda)$ . In the following, we will describe how to construct these elements, which will allow us to effectively optimize the model in the subsequent steps.

Since the measurement space is continuous and infinite, it is impractical to assign a distinct hidden variable  $\lambda$  to every possible measurement setting. Instead, we employ a finite number of hidden variables  $\{\lambda_i\}_{i=1}^{N_{\text{hidden}}}$  and construct a universal response function that can generate outcome probabilities for arbitrary measurements.

For the hidden states  $\sigma(\lambda)$ , each hidden variable  $\lambda$  corresponds to one matrix defined in the Hilbert space of Bob’s subsystem, whose dimensionality is determined by the dimension of that space. To ensure physical validity,

each  $\sigma(\lambda)$  must satisfy  $\sigma(\lambda) \geq 0$  and  $\text{Tr}[\sigma(\lambda)] = 1$ . In practice, directly enforcing these constraints would complicate the optimization process. To circumvent this issue, we adopt a reparameterization scheme by introducing an unconstrained complex matrix  $M_\lambda$  and defining

$$\sigma_\lambda = \frac{M_\lambda M_\lambda^\dagger}{\text{Tr}[M_\lambda M_\lambda^\dagger]},$$

which automatically enforces the positivity and normalization of  $\sigma_\lambda$  throughout the optimization.

To ensure that the response function  $p(a|x, \lambda)$  satisfies the probability constraints  $0 \leq p(a|x, \lambda) \leq 1$  and  $\sum_a p(a|x, \lambda) = 1$ , we define it using a softmax form:

$$p(a|x, \lambda) = \text{softmax}[f_a(x, \lambda)] = \frac{e^{f_a(x, \lambda)}}{\sum_{a'=1}^O e^{f_{a'}(x, \lambda)}},$$

where  $O$  denotes the number of possible outcomes for measurement  $x$ . Here,  $f_a(x, \lambda)$  is a function defined over the measurement space, whose specific form is entirely determined by the hidden variable  $\lambda$ . In the following, we describe the construction of the functions  $f_a(x, \lambda)$ .

### A. The parameterization of the qudit POVM

First, we need to clarify how to parameterize an arbitrary qudit measurement  $M_x$ . Here,  $M_x$  refers to a general POVM consisting of measurement operators  $\{M_{a|x}\}_a$  that satisfy  $M_{a|x} \geq 0$  and  $\sum_a M_{a|x} = I$ . These operators are Hermitian operators of dimension  $d$ , and thus can be expanded in terms of the generalized traceless Gell-Mann matrices  $G_\mu$  and the identity matrix  $I$ : for any Hermitian  $d \times d$  matrix  $M_{a|x}$ , there exists a unique vector  $\vec{g} \in \mathbb{R}^{d^2}$  such that:

$$M_{a|x} = M_{a|x}(\vec{g}) \equiv \frac{1}{\sqrt{2d}} \sum_{\mu=0}^{d^2-1} g_\mu G_\mu. \quad (3)$$

Here we set  $G_0 = \sqrt{\frac{2}{d}}I$  so that:

$$\text{tr}(G_\mu G_\nu) = 2\delta_{\mu\nu}, \quad \text{for all } \mu, \nu \in \{0, 1, 2, \dots, d^2 - 1\}. \quad (4)$$

Hence, for each measurement operator  $M_{a|x} \in M_x$ , there corresponds a unique Gell-Mann vector  $\vec{g}^a \in \mathbb{R}^{d^2}$ .

Since any POVM can be expressed as a convex combination of extremal POVMs, we focus on extremal POVMs for simplicity. As established in Ref. [31], extremal POVMs in  $d$ -dimensional quantum systems contain at most  $d^2$  elements. Considering the completeness constraint of the POVM operators,  $\sum_a M_{a|x} = I$ , an extremal POVM  $M_x$  can be fully parameterized by at most  $(d^2 - 1) \times d^2$  Gell-Mann vector parameters.

### B. The parameterization of the response function

After parameterizing with the Gell-Mann vector  $\vec{g}^a = (g_0, g_1, \dots, g_{d^2-1})$ , the function  $f_a(x, \lambda)$  can be expressed as a function of  $\vec{g}^a$ , denoted as  $f_a(\vec{g}^a, \lambda)$ . We construct a set of orthonormal basis functions  $\{B_m(\vec{g}^a)\}_{m=1}^N$  in the space spanned by  $\vec{g}^a$ , where  $N$  is the number of basis functions. By constructing polynomials based on the space's basis functions, we can approximate any function in the space. This idea was first applied to the construction of the LHV model's response function in Ref. [17]. In our work, we also adopt this polynomial approximation approach, using a finite number of hidden variables to construct a universal response function that can generate corresponding probability distributions for arbitrary measurements. Specifically, the response function can be written as:

$$f_a(\vec{g}^a, \lambda) = \sum_{m=1}^N c_a^m(\lambda) B_m(\vec{g}^a) \quad (5)$$

Here, the coefficients  $c_a^m(\lambda)$  of each orthonormal basis function are determined by the hidden variable  $\lambda$ . Since the hidden variable needs to specify the measurement rules  $\{f_a(\vec{g}^a, \lambda)\}_{a=1}^O$  to obtain different measurement results  $a$ , the hidden variable  $\lambda$  forms an  $M \times N$  matrix:

$$\lambda = \begin{bmatrix} c_1^1(\lambda) & c_1^2(\lambda) & \dots & c_1^{N-1}(\lambda) & c_1^N(\lambda) \\ c_2^1(\lambda) & c_2^2(\lambda) & \dots & c_2^{N-1}(\lambda) & c_2^N(\lambda) \\ \vdots & \vdots & \ddots & \vdots & \vdots \\ c_M^1(\lambda) & c_M^2(\lambda) & \dots & c_M^{N-1}(\lambda) & c_M^N(\lambda) \end{bmatrix}$$

### C. An example: response function for qubit PVMs

To better understand the construction of response function, we take the PVMs for two qubits as an example to elaborate below. In the case of qubits ( $d = 2$ ), the projective measurement  $M_x$  is dichotomic with  $M_x = \{M_{0|x}, M_{1|x}\}$ . Each measurement operator  $M_{a|x}$  can be linearly expressed in terms of Pauli matrices  $\{\sigma_x, \sigma_y, \sigma_z\}$  and the identity matrix  $I$  as:

$$M_{a|x} = \frac{I + (-1)^a (x \cdot \sigma_x + y \cdot \sigma_y + z \cdot \sigma_z)}{2}.$$

Thus, each measurement operator  $M_{a|x}$  can be represented by a Bloch vector  $\vec{g}^a = (x, y, z)$ . The response function  $p(a|x, \lambda)$  then becomes a function constructed from the Bloch vector:

$$\begin{aligned} p(0|x, \lambda) &= \text{softmax}[f_0(\vec{g}^0, \lambda)], \\ p(1|x, \lambda) &= \text{softmax}[f_1(\vec{g}^1, \lambda)], \\ p(0|x, \lambda) + p(1|x, \lambda) &= 1. \end{aligned} \quad (6)$$

Due to the probability normalization condition, it suffices to determine only the measurement rule  $f_0(\vec{g}^0)$ .

Given the properties of dichotomic projective measurements, each measurement operator corresponds to a Bloch vector, and these vectors satisfy the relation  $\vec{g}^1 = -\vec{g}^0$ . Considering that deterministic measurement rules ( $p(a|\cdot) \in \{0, 1\}$ ) already encompass all possible scenarios, we have  $p(1|x, \lambda) = 1 - p(0|x, \lambda)$  on one hand; on the other, the inherent constraints of deterministic rules further restrict the functional form. This leads to the conclusion that the measurement rule function  $f$  satisfies  $f(-\vec{g}^a, \lambda) = 1 - f(\vec{g}^a, \lambda)$ . Based on this, we expand  $f_0(\vec{g}^0)$  in the  $\vec{g}^0$  space using odd spherical harmonics. This approach not only satisfies the odd symmetry requirement but also leverages orthogonality for efficient approximation. By introducing a order  $D$ , we denote the vector composed of odd spherical harmonics up to order  $D$  as  $\vec{B}^D(\vec{g}^0)$  (the specific form for  $D = 3$  is given below):

$$\vec{B}^3(\vec{g}^0) \sim (x, y, z, xyz, \dots, 3x^2y - y^3), \quad (7)$$

$$\vec{g}^0 = (x, y, z).$$

When considering the measurement rule for a single outcome, the hidden variable reduces to a vector  $\vec{\lambda} \in \mathbb{R}^N$  (instead of a matrix), whose dimension is given by:

$$N = \frac{1}{2}(D + 1)(D + 2).$$

To satisfy the requirement of non-vanishing gradients in numerical optimization, we employ a sigmoid function to transform the mapping into probabilistic form:

$$p(0|x, \lambda) = \text{sigmoid} \left[ \sum_{m=1}^N \vec{B}_m^D(\vec{g}^0) \cdot \vec{\lambda} \right], \quad (8)$$

$$\text{sigmoid}[y] = \frac{1}{1 + e^{-y}}.$$

#### IV. OPTIMIZATION OF LHS MODEL THROUGH LOSS FUNCTION MINIMIZATION

In the previous section, we established that the LHS model is determined by the hidden-variable matrix  $\lambda$  and the hidden state  $\sigma(\lambda)$ . To determine whether a given entangled state  $\rho$  is steerable, we need to optimize the sets of hidden variables  $\{\lambda_1, \lambda_2, \dots, \lambda_{N_{\text{hidden}}}\}$  and hidden states  $\{\sigma(\lambda_1), \sigma(\lambda_2), \dots, \sigma(\lambda_{N_{\text{hidden}}})\}$  to find the optimal LHS model. If the optimal LHS model, under different measurement settings  $M_x$ , can reproduce the quantum assemblage  $\{\sigma_{a|x}^{QM}\}_{a=1}^O$ , with each measurement setting comprising  $O$  measurement operators  $M_{a|x}$ , then the state is unsteerable. To this end, we first introduce a loss function to quantify the discrepancy between LHS assemblages and quantum assemblages, and then show how this loss can be minimized through gradient-based optimization to obtain an optimal LHS model.

#### A. Loss function

To quantify the difference between the two assemblages  $\{\sigma_{a|x}^{LHS}\}$  and  $\{\sigma_{a|x}^{QM}\}$  for a fixed measurement setting  $M_x$ , we begin by defining a distance measure  $D_{\text{meas}}$ . The trace distance is a metric to distinguish two density operators  $\rho$  and  $\rho'$ , i.e.,  $D_Q(\rho, \rho') = \frac{1}{2}\|\rho - \rho'\|$ , where  $\|X\| := \text{tr}[|X|]$  is the trace norm [32]. Similarly, we can define the distance between two assemblages as:

$$D \left[ \{\sigma_{a|x}^{LHS}\}_{a=1}^O, \{\sigma_{a|x}^{QM}\}_{a=1}^O \right] = \sum_{a=1}^O D_Q \left( \sigma_{a|x}^{LHS}, \sigma_{a|x}^{QM} \right). \quad (9)$$

Any valid distance metric ( $D_{\text{meas}} \geq 0$  with  $D_{\text{meas}} = 0$  if and only if the assemblages are identical) may be utilized, provided it is differentiable with respect to the individual components. Mathematically, our objective is to minimize  $D \left[ \{\sigma_{a|x}^{LHS}\}_{a=1}^O, \{\sigma_{a|x}^{QM}\}_{a=1}^O \right]$  simultaneously across all possible measurement settings  $M_x$ . The free parameters in this optimization are the hidden variables  $\{\lambda_1, \lambda_2, \dots, \lambda_{N_{\text{hidden}}}\}$  and hidden states  $\{\sigma(\lambda_1), \sigma(\lambda_2), \dots, \sigma(\lambda_{N_{\text{hidden}}})\}$ , which together constitute the LHS assemblage  $\sigma_{a|x}^{LHS}$ . Drawing upon machine learning terminology, this minimization can be formulated as optimizing a scalar loss function:

$$\mathcal{L}(\text{LHS} || \text{QM}) = \left\langle D \left[ \{\sigma_{a|x}^{LHS}\}_{a=1}^O, \{\sigma_{a|x}^{QM}\}_{a=1}^O \right] \right\rangle_{M_x}. \quad (10)$$

This is a single non-negative number: the mean deviation of  $\{\sigma_{a|x}^{LHS}\}_{a=1}^O$  from  $\{\sigma_{a|x}^{QM}\}_{a=1}^O$  over all possible measurement settings  $M_x$ . In this way, we treat all measurement choices as equally important. A loss function  $\mathcal{L} = 0$  indicates that the quantum assemblages obtained under all possible measurements can be reproduced by the LHS model. Then, the quantum state  $\rho$  is unsteerable.

#### B. Optimization Via Stochastic Gradient Descent

Our objective is to minimize the loss function defined above, thereby determining whether a given quantum state admits an LHS model and is thus unsteerable. Since the loss function involves an average over a continuous space of measurement settings, it is generally intractable to evaluate it exactly. Instead, we adopt a stochastic optimization strategy: at each iteration, a finite batch of measurement settings is randomly sampled to approximate the loss and its gradient. By repeatedly updating the model parameters based on these sampled measurements, the optimization effectively explores the entire measurement space. Below, we describe the complete iterative optimization procedure in detail.

### (i) Parameter Initialization.

The procedure requires the entangled state  $\rho$ , the system dimensions (number of qudits  $N$  and single-qudit dimension  $d$ ), the model precision (polynomial order  $D$  of the orthonormal basis), and training configurations including the number of hidden variables  $N_{\text{hidden}}$ , total steps  $N_{\text{steps}}$ , measurements per step  $N_{\text{meas/step}}$ , and learning rate  $\eta$ .

### (ii) Model Preparation.

This step prepares the quantum assemblages and response functions. The quantum assemblages  $\{\sigma_{a|x}^{QM}\}$  are obtained by randomly sampling  $N_{\text{samples}}$  measurements  $M_x$  and computing their corresponding unnormalized post-measurement states. Concurrently, the measurement response function  $p(a|x, \lambda)$  is parameterized using the  $N_{\text{basis\_dim}}$ -dimensional orthonormal basis functions  $\vec{B}^D(\vec{g})$ , where  $N_{\text{basis\_dim}}$  is determined by  $D$  and represents the number of terms in the orthonormal basis, constructed from the Gell-Mann coefficient vectors  $\vec{g}^a$  of the sampled measurement operators, via softmax  $[f_a(x, \lambda)]$ .

### (iii) LHS Model Assembly.

The LHS model is built using two sets of parameters: the hidden-variable  $\lambda$  with shape  $(N_{\text{hidden}}, N_{\text{basis\_dim}})$  and the hidden state  $\sigma(\lambda)$  with shape  $(N_{\text{hidden}}, \sigma_{\text{param\_dim}})$ , where  $\sigma_{\text{param\_dim}} = d_{\text{Bob}}^2$  and  $d_{\text{Bob}} = d^{N-1}$ . The LHS assemblage is formed by averaging the post-measurement states over all hidden variables:

$$\sigma_{a|x}^{LHS} = \frac{1}{N_{\text{hidden}}} \sum_{\lambda} p(a|x, \lambda) \cdot \sigma(\lambda).$$

### (iv) Gradient-Based Optimization.

We use the gradient descent algorithm [33, 34] to minimize the loss function defined as

$$\mathcal{L} = \frac{1}{N_{\text{meas/step}}} \sum_{\text{meas}} D \left( \{\sigma_{a|x}^{LHS}\}_{a=1}^O, \{\sigma_{a|x}^{QM}\}_{a=1}^O \right)$$

The basic idea is as follows: we parameterize the loss function in terms of parameters  $\theta = (\lambda, \sigma)$ . After random initialization of these parameters, they are adjusted iteratively. In each iteration,  $N_{\text{meas/step}}$  new measurements are sampled, and the gradients  $\nabla_{\lambda} \mathcal{L}$  and  $\nabla_{\sigma} \mathcal{L}$  are computed via automatic differentiation. The parameters are then updated according to

$$\theta_{\text{new}} = \theta_{\text{old}} - \eta \nabla_{\theta} \mathcal{L}(\theta_{\text{old}}), \quad (11)$$

which, for a sufficiently small learning rate  $\eta > 0$ , reduces the loss (as can be verified by a first-order expansion of  $\mathcal{L}(\theta_{\text{new}})$  with respect to  $\eta$ ). This process cycles through  $N_{\text{steps}}$  iterations until convergence.

### (v) Result Output and Steerability Certification.

The algorithm outputs the optimized parameters  $\lambda_{\text{opt}}$  and  $\sigma_{\text{opt}}$ . When the final loss value converges close to zero, it indicates the successful construction of a valid LHS model, thereby certifying the state as unsteerable.

The algorithm becomes stochastic because we cannot compute the exact average over the full continuum of measurement settings in the loss function. Instead, at each update step, we sample a new, large but finite batch of settings  $(M_1, M_2, \dots, M_{N_{\text{meas}}})$  and replace the exact mean with a Monte Carlo estimate to approximate both the average deviation and its gradient.

## V. THE APPLICATIONS

To validate the effectiveness of the proposed method, we apply it to assessing the steerability of two-qubit Werner states and two-qutrit isotropic states under different measurement scenarios.

### A. Two-qubit werner states

We take the two-qubit Werner state as an example:

$$\rho(v) = v|\psi^-\rangle\langle\psi^-| + \frac{(1-v)}{4}I_2 \otimes I_2, \quad (12)$$

$$|\psi^-\rangle = \frac{1}{\sqrt{2}}(|01\rangle - |10\rangle).$$

The parameter  $v \in [0, 1]$  represents the visibility of the singlet. It is known that these states are separable for  $v \leq 1/3$  [35]. As the parameter  $v$  decreases from 1 to 0, the quantum state gradually transitions from a maximally entangled state to a completely separable state, and its steerability correspondingly changes from “steerable” to “unsteerable”.

For the entangled state, its steering properties may differ across different measurement scenarios. To this end, the following will examine the critical value of  $v$  under three different measurement scenarios, including: three fixed Pauli measurements, arbitrary PVMs, and arbitrary POVMs.

#### 1. The Three fixed Pauli Measurements

Theoretical analysis shows that when Alice employs the three Pauli measurements  $X$ ,  $Y$ , and  $Z$ , the corresponding steering inequality for this system is:

$$\langle XX \rangle + \langle YY \rangle + \langle ZZ \rangle \leq \sqrt{3}.$$

This inequality gives a clear steering threshold: the Werner state is unsteerable when  $v \leq 1/\sqrt{3}$  [30].

We apply our method to analyze the steerability of this quantum state under three fixed measurements. We construct an LHS model for the assemblages on Bob’s side. Here, Alice performs three fixed measurements, eliminating the need for random measurement sampling during training to obtain optimal parameters. The loss

function only needs to average over these three measurements. Our numerical results accurately reproduce the theoretical critical point  $v_c = \frac{1}{\sqrt{3}}$ , as shown in the Fig. 2.

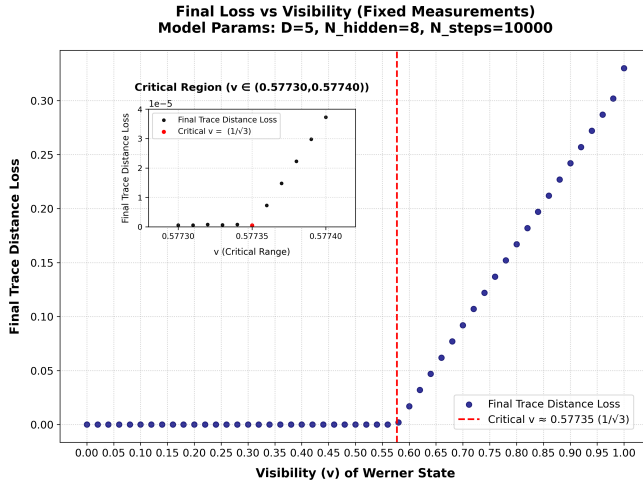


FIG. 2: Steerability of the two-qubit Werner states under three Pauli measurements. The parameters adopted for optimizing the LHS model are as follows: the order of orthonormal basis functions  $D = 5$ , the number of hidden variables  $N_{\text{hidden}} = 8$ , and the number of gradient descent iterations  $N_{\text{steps}} = 10^5$ . Theoretically, the higher the order  $D$  of the orthonormal basis functions and the more gradient descent iterations, the higher the result accuracy. However, practical verification shows that the currently selected parameters are sufficient to meet the requirements.

## 2. The Arbitrary PVMs

LHS models constructed based on a finite set of measurements (e.g., three Pauli measurements) cannot provide a complete criterion for the steerability of quantum states. The threshold obtained under such limited measurements ( $v_c = 1/\sqrt{3}$ ) is far from optimal. Next, we consider more PVMs, which are experimentally feasible to implement. Their measurement operators must satisfy hermiticity  $M_{a|x}^\dagger = M_{a|x}$ , positive semi-definiteness  $M_{a|x} \geq 0$ , idempotency  $M_{a|x}^2 = M_{a|x}$ , and orthogonality  $M_{a|x} M_{a'|x} = \delta_{a,a'} M_{a|x}$ .

We perform uniform random sampling over the entire space of qubit PVMs. At each step of the gradient descent, we resample a new batch of PVMs. Theoretically, when the number of optimization steps and sample size are sufficiently large, this strategy can effectively approximate coverage of the entire continuous measurement space. For the quantum assemblages generated by sampling, we simultaneously optimize the hidden variables  $\lambda$  and hidden states  $\sigma(\lambda)$  to find the optimal local hidden-state model. To rigorously verify the universality of the obtained model and ensure it is not merely tailored

to the finite training measurement set, we compute the loss function on an independent test set. Our numerical results confirm the theoretical conclusion: for two-qubit Werner states, the assemblages generated under PVMs admit an LHS model up to  $v = \frac{1}{2}$  (see Fig. 3).

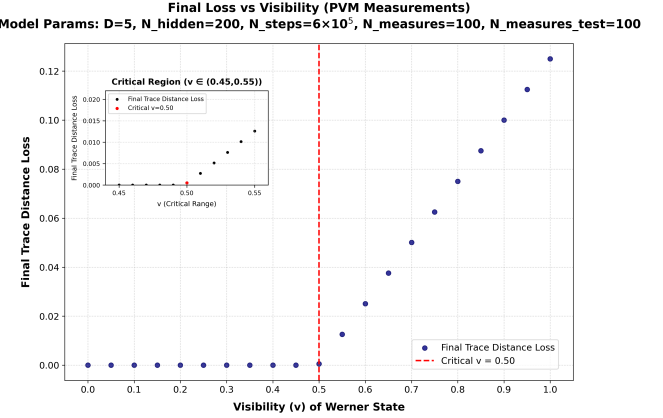


FIG. 3: Steerability of the two-qubit Werner states under PVMs. The parameters adopted for optimizing the LHS model are as follows: the order of orthonormal basis functions  $D = 5$ , the number of hidden variables  $N_{\text{hidden}} = 200$ , and the number of gradient descent steps  $N_{\text{steps}} = 6 \times 10^5$ . To verify that the optimal LHS model is not only applicable to the measurements used in training, we uniformly and randomly sampled a batch of measurements for testing, which confirms the model's universality.

## 3. The Arbitrary POVMs

POVMs represent a special case of generalized POVMs. The existence of non-projective POVMs enables quantum theory to generate statistical predictions that cannot be simulated using only projective measurements and classical randomness [31]. Therefore, restricting quantum steering research solely to PVMs is incomplete. We next investigate the steerability of entangled states under the more general POVMs, where the measurement operators  $M_{a|x}$  satisfy hermiticity  $M_{a|x}^\dagger = M_{a|x}$  and positive semi-definiteness  $M_{a|x} \geq 0$ .

Our method is the first numerical approach to verify the critical value  $v = 1/2$  for the steerability of two qubit werner states via the construction of an LHS model under POVMs (see Fig. 4). Under the configuration of Python 3.12, CUDA 12.4, and an RTX 4090 GPU, obtaining the optimal LHS model for the entangled state corresponding to each  $v$  value requires one hour of computation per run.

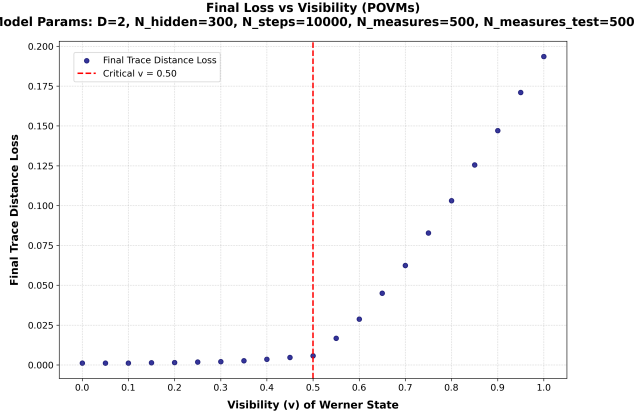


FIG. 4: Steerability of the two-qubit Werner states under POVMs. The parameters adopted for optimizing the LHS model are as follows: the order of orthonormal basis functions  $D = 2$ , the number of hidden variables  $N_{\text{hidden}} = 300$ , and the number of gradient descent steps  $N_{\text{steps}} = 10^5$ . At each step of the gradient descent,  $N_{\text{measures}}$  measurements are randomly selected to optimize the parameters, yielding the optimal  $\lambda$  and  $\sigma(\lambda)$ . Finally, the loss value is computed using  $N_{\text{measures\_test}}$  measurements.

### B. Two-qutrit isotropic states

We investigate the steerability of bipartite qutrit states under PVMs and POVMs. Specifically, we consider isotropic states of the form:

$$\rho = v|\psi^+\rangle\langle\psi^+| + \frac{(1-v)}{9}I_3 \otimes I_3, \quad (13)$$

$$|\psi^+\rangle = \frac{1}{\sqrt{3}}(|00\rangle + |11\rangle + |22\rangle).$$

The  $|\psi^+\rangle$  denotes the maximally entangled isotropic state. It is well known that these states are entangled for  $v > \frac{1}{4}$ , and are steerable under PVMs for  $v > \frac{5}{12}$  [19].

For the case of PVMs, our numerical results indicate that the steering transition occurs at a critical value of  $v = 0.42$ , which is in very close agreement with the known theoretical bound  $v > \frac{5}{12}$ . For general POVMs, we observe that the growth rate of the loss function increases significantly for  $v > 0.3$ , with a further acceleration occurring beyond  $v > 0.4$  (see Fig. 5). Based on this observed trend, we conjecture that the steering threshold under general POVMs is close to  $v \approx 0.3$ . This indicates that, compared with PVMs, POVMs possess a certain advantage in detecting the steerability of such high-dimensional quantum states.

The achievable numerical precision in our approach is constrained by computational resources. This limitation mainly arises from the fact that, in high-dimensional systems, the increase in the number of measurement outcomes requires the introduction of a larger set of orthonormal basis functions for their description, which sig-

nificantly enlarges the matrix size associated with each hidden variable  $\lambda$ , thereby making the numerical optimization considerably more challenging. In our computational environment (Python 3.12, CUDA 12.4, NVIDIA RTX 4090 GPU), a single optimization run to obtain the optimal local hidden-state model for a given visibility  $v$  typically requires several tens of hours of computation.

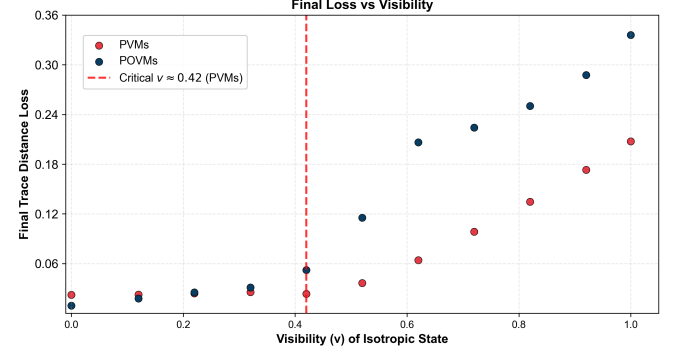


FIG. 5: Steerability of the two-qutrit isotropic states under PVMs and POVMs. Red points show results under PVMs, with the following parameters: order of orthonormal basis functions  $D = 2$ , number of hidden variables  $N_{\text{hidden}} = 100$ , number of gradient descent steps  $N_{\text{steps}} = 2 \times 10^5$ , and  $N_{\text{meas}} = 200$  randomly selected measurements per gradient step. Blue points correspond to results under general POVMs, with parameters:  $D = 3$ ,  $N_{\text{hidden}} = 200$ ,  $N_{\text{steps}} = 2 \times 10^5$ , and  $N_{\text{meas}} = 300$ .

## VI. CONCLUSION

In this work, we propose a machine learning-based framework for constructing an LHS model to determine the steerability of a given entangled state under arbitrary measurements. This framework adopts the commonly used batch sampling concept in machine learning, where a new batch of measurements is sampled at each step of the gradient descent process. The response function for each measurement is represented by expanding it in orthonormal basis polynomials in the measurement space. This idea was first applied to the construction of local hidden-variable models in Ref. [17]. We introduce an unconstrained complex matrix  $M_\lambda$  and map it to a valid hidden-state  $\sigma(\lambda)$  through parameter reparameterization. Using these steps, we construct an LHS model for each batch of measurements. We then define the trace distance between the LHS assemblages and the quantum assemblages as the loss function, which is minimized using gradient descent to iteratively update the parameters of the LHS model. After repeated optimization steps, the framework ultimately converges to an optimal LHS model that is applicable to any measurement. When the loss function converges to zero, it indicates that the opti-

mal LHS model has successfully reproduced the target quantum assemblages, thereby certifying the quantum state as unsteerable.

To validate the effectiveness of our method, we apply it to analyze the steerability of two-qubit Werner states and two-qutrit isotropic states. For two-qubit Werner states, under three Pauli measurements [30], arbitrary PVMs [20], and arbitrary POVMs [22], our method is the first to obtain numerical visibility bounds that are simultaneously consistent with the known analytical results among existing numerical approaches [23, 24, 29]. For two-qutrit isotropic states, our method reaches the known analytical visibility bound under arbitrary PVMs [19]. In addition, we further explore the steerability visibility of these states under POVMs. Due to limitations in computational resources, we conjecture that the critical visibility is approximately  $v = 0.3$ . This provides further evidence that POVMs offer an advantage over PVMs in revealing the steerability of such states.

In principle, the accuracy of our constructed LHS model can be further improved by increasing key parameters, such as the polynomial expansion order  $D$ , the number of hidden variables  $N_{\text{hidden}}$ , and the number of gradient descent steps  $N_{\text{steps}}$ . However, such improvements in accuracy are typically accompanied by a significant increase in computational cost. With the future development of more efficient optimization algorithms and the continuous growth of computational resources, the numerical framework proposed in this work is expected to enable more precise and broader applications in the study of quantum steering.

## ACKNOWLEDGMENT

This work is supported by the National Natural Science Foundation of China (Grants No. 62571060, No. 62171056, and No. 62220106012).

---

[1] R. Horodecki, P. Horodecki, M. Horodecki, and K. Horodecki, *Rev. Mod. Phys.* **81**, 865 (2009).

[2] S. J. Freedman and J. F. Clauser, *Phys. Rev. Lett.* **28**, 938 (1972).

[3] A. Aspect, P. Grangier, and G. Roger, *Phys. Rev. Lett.* **47**, 460 (1981).

[4] A. Einstein, B. Podolsky, and N. Rosen, *Phys. Rev.* **47**, 777 (1935).

[5] A. Acín, N. Brunner, N. Gisin, S. Massar, S. Pironio, and V. Scarani, *Phys. Rev. Lett.* **98**, 230501 (2007).

[6] U. Vazirani and T. Vidick, *Phys. Rev. Lett.* **113**, 140501 (2014).

[7] Y.-A. Shih, W.-G. Chang, G. N. M. Tabia, H.-C. Weng, T.-Y. Tsai, C.-S. Chuu, H.-Y. Ku, and C. Budroni, *Phys. Rev. Res.* **7**, L032035 (2025).

[8] H. Kang, J. F. Kam, G. J. Mooney, and L. C. Hollenberg, *Phys. Rev. Appl.* **23**, 014057 (2025).

[9] S. Pironio, A. Acín, S. Massar, A. B. de la Giroday, D. N. Matsukevich, P. Maunz, S. Olmschenk, D. Hayes, L. Luo, T. A. Manning, and C. Monroe, *Nature* **464**, 1021 (2010).

[10] S. Pironio and S. Massar, *Phys. Rev. A* **87**, 012336 (2013).

[11] M. L. Almeida, S. Pironio, J. Barrett, G. Tóth, and A. Acín, *Phys. Rev. Lett.* **99**, 040403 (2007).

[12] R. Augusiak, M. Demianowicz, J. Tura, and A. Acín, *Phys. Rev. Lett.* **115**, 030404 (2015).

[13] J. Bowles, J. Francfort, M. Fillettaz, F. Hirsch, and N. Brunner, *Phys. Rev. Lett.* **116**, 130401 (2016).

[14] D. J. Saunders, S. J. Jones, H. M. Wiseman, and G. J. Pryde, *Nat. Phys.* **6**, 845 (2010).

[15] R. F. Werner, *Phys. Rev. A* **40**, 4277 (1989).

[16] M. T. Quintino, T. Vértesi, D. Cavalcanti, R. Augusiak, M. Demianowicz, A. Acín, and N. Brunner, *Phys. Rev. A* **92**, 032107 (2015).

[17] N. von Selzam and F. Marquardt, *PRX Quantum* **6**, 020317 (2025).

[18] E. Schrödinger, *Mathematical Proceedings of the Cambridge Philosophical Society* **31**, 555 (1935).

[19] H. M. Wiseman, S. J. Jones, and A. C. Doherty, *Phys. Rev. Lett.* **98**, 140402 (2007).

[20] J. Bowles, F. Hirsch, M. T. Quintino, and N. Brunner, *Phys. Rev. A* **93**, 022121 (2016).

[21] H. C. Nguyen and O. Gühne, *Phys. Rev. A* **101**, 042125 (2020).

[22] Y. Zhang and E. Chitambar, *Phys. Rev. Lett.* **132**, 250201 (2024).

[23] D. Cavalcanti, L. Guerini, R. Rabelo, and P. Skrzypczyk, *Phys. Rev. Lett.* **117**, 190401 (2016).

[24] F. Hirsch, M. T. Quintino, T. Vértesi, M. F. Pusey, and N. Brunner, *Phys. Rev. Lett.* **117**, 190402 (2016).

[25] D.-L. Deng, *Phys. Rev. Lett.* **120**, 240402 (2018).

[26] P. Wang, Z. Li, and H. Meng, *Phys. Rev. A* **112**, 042414 (2025).

[27] X. Lin, Z. Chen, and Z. Wei, *Phys. Rev. A* **107**, 062409 (2023).

[28] T. Kriváčky, Y. Cai, D. Cavalcanti, A. Tavakoli, N. Gisin, and N. Brunner, *npj Quantum Information* **6**, 70 (2020).

[29] M. Li, Y. Jia, F. Guo, H. Dong, S. Qin, and F. Gao, *Phys. Rev. A* **111**, 052446 (2025).

[30] E. G. Cavalcanti, S. J. Jones, H. M. Wiseman, and M. D. Reid, *Phys. Rev. A* **80**, 032112 (2009).

[31] G. M. D'Ariano, P. Lo Presti, and P. Perinotti, *Journal of Physics A: Mathematical and General* **38**, 5979 (2005).

[32] H.-Y. Ku, S.-L. Chen, C. Budroni, A. Miranowicz, Y.-N. Chen, and F. Nori, *Phys. Rev. A* **97**, 022338 (2018).

[33] P. Mehta, M. Lukin, C.-H. Wang, A. G. Day, C. Richardson, C. K. Fisher, and D. J. Schwab, *Physics Reports* **810**, 1 (2019), a high-bias, low-variance introduction to Machine Learning for physicists.

[34] F. Marquardt, *SciPost Phys. Lect. Notes* **29** (2021).

[35] A. Peres, *Phys. Rev. Lett.* **77**, 1413 (1996).